Cellular and Molecular Life Sciences (2026) 83:220
https://doi.org/10.1007/s00018-026-06178-1

ORIGINAL ARTICLE

Cytoplasmic cyclin D1 modulates brain cortex development

Neus Pedraza[1] · Daniel Rocandio[1] · Bahira Zammou[1] · Maria Ventura Monserrat[1] · Ariadna Ortiz-Brugués[1] · Pau Marfull-Oromí[1] · Disha Chauhan[1] · Mario Encinas[1] · Xavier Dolcet[1] · Francisco Ferrezuelo[1] · Eloi Garí[1] · Joaquim Egea[1]

Received: 21 July 2025 / Revised: 3 March 2026 / Accepted: 4 March 2026
© The Author(s) 2026

Abstract

During nervous system development, the interplay between cell cycle regulation and neurogenesis is fundamental to achieving the correct timing for neuronal differentiation. However, the molecules regulating this transition are poorly understood. Among these, the cell-cycle regulatory cyclins and their cyclin-dependent kinases (CDKs) play a pivotal role. In the present work we uncover an unknown function of cyclin D1 (CCND1) during cortex development which is independent of cell cycle regulation and that relies on its cytoplasmic localization and membrane association. We show that CCND1 is localized in the cytoplasm of the radial glial process (RGP) of neuron progenitors in different regions of the developing brain, including the pallium. Cytoplasmic CCND1 is enriched at the distal tip of the RGP, adjacent to the meningeal basement membrane, and overlaps with β1-integrin at the plasma membrane. *Ccnd1* knock-out embryos show an abnormal cortical layering in which the distribution of TBR2+and CTIP2+cells are affected without displaying proliferation defects. This is consistent with a cytoplasmic function of CCND1 as overexpression by in utero electroporation of a dominant negative CCND1, unable to activate CDKs, and targeted to the cytoplasmic membranes, reproduces some of these TBR2 and CTIP2 defects. Finally, we provide evidence that cytoplasmic CCND1 affects neuron morphology and that it is required for the proper detachment of the RGP from the meningeal basement membrane by a mechanism involving the phosphorylation of the integrin effector protein paxillin. Hence, we propose that CCND1 has an important cytoplasmic function for cortical development independently of cell cycle regulation.

Keywords Radial glial cells · End-feet adhesion · Neuron migration · Neuritogenesis · In utero electroporation

Neus Pedraza and Daniel Rocandio contributed equally to the work and are considered first authors.

Significant Statement A key developmental step during nervous system formation is the transition from proliferating progenitors to postmitotic neurons. However, the molecular mechanisms regulating this process are not fully understood. Cyclin D1 (CCND1) is a canonical regulator of cell cycle in the cell nucleus. Surprisingly, we show that CCND1 is also located in the radial glial process of neuron progenitors and associated to the plasma membrane in different regions of the developing mouse brain. We uncover a novel function for this cytoplasmic CCND1 and show that it is required for proper cortical layering, independent of cell cycle regulation. Mechanistically, we provide evidence that this function is mediated by the integrin effector paxillin. We propose therefore that cytoplasmic CCND1 is important for cortex development independent of cell cycle regulation.

✉ Neus Pedraza
neus.pedraza@udl.cat

✉ Joaquim Egea
joaquim.egea@udl.cat

[1] Departmet of Basic Medical Sciences, Universitat de Lleida/ Institut de Recerca Biomèdica de Lleida (IRBLLEIDA), Avda. Rovira Roure, 80, 25198 Lleida, Spain

Published online: 14 April 2026

Introduction

Projection neurons within the cerebral cortex are organized in a six-layered structure, each one with specific molecular identities and functions. During development, these neurons differentiate from proliferative progenitor cells in the ventricular zone (VZ, apical progenitors) or in the subventricular zone (SVZ, basal progenitors). Cell cycle regulation plays an important role during neuron differentiation. Symmetric divisions give rise to two daughter cells that maintain the progenitor status whereas in asymmetric, neurogenic divisions, one of the daughter cells exits the cell cycle and differentiates into a postmitotic neuron which finally migrates towards the cortical plate (CP) and populates a specific cortical layer [7]. Proliferative versus neurogenic divisions are determined by the duration of the G1 phase of the cell cycle so that the lengthening of the G1 phase stimulates neurogenesis by promoting neurogenic divisions [28, 38, 50]. However, the exact mechanisms that control the balance between cell renewal and lineage commitment are still poorly understood.

D-type cyclins (CDND1-3) control cell cycle length by acting as regulatory subunits of cyclin-dependent kinases (CDKs) 4 and 6. CCND/CDK complexes inhibit the pRB repressor by phosphorylation, releasing the E2F transcription factor and promoting the expression of genes necessary for cell cycle entry [45]. Overexpression of CCND1/CDK4 promotes G1 shortening, expansion of neural progenitors and a delay of neurogenesis [1, 26], and alterations in CCND1 levels in neural progenitors have been related to cortical defects in Down syndrome [35]. These results are in contrast with observations in *Ccnd1* knock-out animals which do not display proliferation defects in the neocortex [16], and just mild defects in the cerebellum that lead to a reduction of cerebellar size [40]. Nevertheless, deficient *Ccnd1* mice show symptoms of neurological impairment as indicated by an abnormal hindlimb clasping reflex, although the underlying causes have not yet been established [46]. In addition, genetic variants of the *CCND2* gene in humans that produce a gain-of-function protein have been associated to polymicrogyria and megalencephaly [21, 32] while loss-of-function variants have been linked to microcephaly in humans [39] and in mice [16, 22].

Non-canonical functions of CCNDs/CDKs have been reported [23]. CCND1/CDKs can directly regulate the activity of transcription factors such as ATOH1 or HES6 and control neuronal commitment in a cell-cycle independent manner [29, 33]. Interestingly, CCND1 has also been reported to be associated to the plasma membrane and regulate cytoplasmic targets such as β1-integrin and its downstream effector paxillin and affects cell migration and cell–matrix adhesion [9, 12]. Cytoplasmic-associated CCND1 activity is also relevant for neural communication as it regulates gamma-aminobutyric acid (GABA) signaling in rat hippocampal neurons [37].

In the present work, we demonstrate that CCND1 is expressed in the cytoplasm of radial glial cells in the developing cortex overlapping with b1-integrin at the plasma membrane of the tip of the radial glial process (RGP). *Ccnd1* knock-out animals display an abnormal cortical layering of TBR2 + and CTIP2 + neurons, but this phenotype is not accompanied by proliferation effects. Instead, some aspects of these cortical layering defects are reproduced when a cytoplasmic dominant negative CCND1 is overexpressed by in utero electroporation, suggesting a function for cytoplasmic CCND1 in cortical layering. Mechanistically, we suggest that this cytoplasmic CCND1 affects neuron morphology both in vivo and in vitro, and that it is important for the proper detachment of the RGP from the meningeal basement membrane through the phosphorylation of the integrin signaling complex effector, paxillin. Therefore, we propose that CCND1 has an important cytoplasmic function in cortex development that is separate from its role in regulating the cell cycle.

Materials and methods

Mice

Animal care followed the Guidelines of the University of Lleida for Animal Experimentation in accordance with Catalan, Spanish, and European Union regulations (Decret 214/1997, Real Decreto 53/2013, and Directive 63/2010). Animals were housed in the animal care facility of the University of Lleida with 12:12 h light/dark cycle and food/water available ad libitum. *Ccnd1* knock-out mice [46] were obtained from Charles-River and backcrossed to C57/bl6 background. For embryo dissection, the day on which the vaginal plug was found was considered as embryonic (E) day 0.5 and the date of birth was considered as postnatal (P) day 0. PCR genotyping was done by tail biopsy using the following primers: common primer CTGTCGGCGCA GTAGCAGAGAGCTACAGAC, *Ccnd1* wild-type allele specific primer CGCACAGGTCTCCTCCGTCTTGAGCA TGGC and a *Ccnd1* knock-out specific primer CTAGTGA GACGTGCTACTTCCATTTGTCACG. The expected band sizes are 249 bp for the WT allele and 394 bp for the *Ccnd1* knock-out allele.

Expression vectors

One copy of His tag or three copies of the HA epitope were added at 5' end of the human *CCND1* or mouse *Cdk4* open

reading frames (ORF). *CCND1*^{CAAX} or *Cdk4*^{CAAX} constructs are fusions of the 3′ end of the K-Ras ORF containing the CAAX motif (GGC TGT GTG AAA ATT AAA AAA TGC ATT ATA ATG TAA) at the 3′ end of the *CCND1* or *Cdk4* ORFs (Fusté et al., 2016b). Standard PCR-mediated site-directed mutagenesis was used to obtain the K112E mutant of *CCND1* [9]. Mouse wild-type and non-phosphorylatable paxillin were previously described [12]. Constructs were subcloned into the expression vectors pcDNA3 or pCAGIC (Addgene, 11159). pcDNA3 was used for neuron transfection in vitro and was co-transfected with pEGFP-N1 plasmid (Clontech) to assess neuron morphology. pCAGIG contains an internal ribosome entry site (IRES) and the EGFP gene for tracking electroporated cells in the in utero electroporation experiments (IUE).

Intraventricular injection and in utero electroporation

E13.5-E15.5 pregnant CD1 wild-type mice were deeply anesthetized with isoflurane (IsoFlo, Zoetis) during the entire operation procedure. To relax uterus muscles, β2 agonist Ritodrine (Sigma R0758) was administered intraperitoneally, and buprenorphine (Buprex, 100 mg/ml) subcutaneously as an analgesic. A 2 cm laparotomy section was made in the abdomen, and the uterine horns were carefully exposed and lubricated with NaCl 0.9% at 37º C. Two to 4 µl of purified plasmid DNA dissolved in PBS (1 µg/µl) containing 0.025% of Fast Green (Sigma-Aldrich) was injected in the lateral ventricles of each embryo using a glass capillary (World Precision Instruments) sharpened previously by Puller P-97 (Sutter Instrument). Platinum electrodes (CUY701P20L, Nepagene) were placed across the head with the positive pole adjacent to the pallium, to enhance the permeability of the cell membrane and allow the entrance of DNA. Five 30 mV electric pulses of 50 ms with intervals of 950 ms were charged by an electroporator (ECM830, BTX). Uterine horns were placed back into the abdominal cavity and abdomen wall and skin were surgically sutured. During the whole operation embryos were manipulated with ring forceps (Fine Science Tools). Embryonic brains were dissected, as indicated, at different timepoints after electroporation and fixed directly in ice cold 4% paraformaldehyde (PFA) solution in PBS overnight. Postnatal brains were obtained after intracardiac perfusion with ice-cold PBS and ice-cold 4% PFA-PBS and post-fixed overnight in ice-cold 4% PFA-PBS.

EdU labeling

E14.5 pregnant mice were injected intraperitoneally with 100 µg/g body weight of EdU (ThermoFisher, C10337) using a stock solution of 10 mg/ml in PBS. Pregnant mice were sacrificed 1 h later and the embryonic brains were processed for cryosectioning (see below) and reacted with the fluorescent dye through click chemistry according to manufacturer instructions. Sections were washed with PBS and permeabilized and blocked with 5% goat serum in 0.1% Triton X-100 in PBS for 1 h at room temperature. Subsequently, the slides were incubated during 30 min with Click-iT reaction cocktail (ThermoFisher, C10337) protected from light. After washing, DAPI was added to sections during 2 h at room temperature for nuclei staining.

Cortical neuron culture and neurite analysis

Primary culture of cortical neurons from E15.5 *Ccnd1* knock-out, control littermates or wild-type embryos were prepared as previously described [37]. To identify the different genotypes, a PCR reaction was set-up during the dissection procedure using a tail biopsy as indicated above. Primary cortical neurons were electroporated using Ingenio electroporation solution (Mirus) following the manufacturer's recommendations and the proportion 2 µg DNA:2*10^6 cells. The media was changed 2 h after transfection and cells were fixed at 1–4 days in vitro (DIV). For *Ccnd1* down-regulation, scrambled shRNA (SHC002, Sigma) or *Ccnd1* shRNA (TRCN0000026883, Sigma) were co-transfected with EGFP-N1 in a proportion 2:1, by in-tube transfection as described previously [19] with Lipofectamine 2000 (ThermoFisher). For neurite analysis, cortical neurons were fixed using 4% PFA and 4% sucrose in PBS for 15 min at room temperature and then washed with PBS. Neurons were permeabilized for 5 min with 0.1% Triton X-100 in PBS and blocked with 3% BSA in PBS. Primary antibodies α-GFP (ThermoFisher, A11120), α-cleaved caspase-3 (Cell Signaling, 9661) or α-HA (Sigma, 3F10) were diluted 1:200 in 0.3% BSA-PBS. Proteins were detected by incubation with fluorescent-labelled secondary antibodies (ThermoFisher). Hoechst (Sigma) was used to label the nuclei. Immunofluorescence images were obtained with an Olympus IX71 microscope and quantification of neurite length was performed using NeuronJ of ImageJ. All the analysis were done blind to the experimental condition.

Lentiviral production and MEF infection

For lentivirus production, HEK293T cells were transfected with lentiviral expression vectors, envelope plasmid pVSV.G, and packaging plasmid pHR'82ΔR at a ratio of 2:1:1. For RNA interference, the *Ccnd1* MISSION shRNA TRCN0000026883 and the control SHC002 cloned in a pLKO.1-puro were obtained from Sigma-Aldrich.

MEFs (mouse embryonic fibroblasts) were infected and selected with Puromycin.E

Tissue immunofluorescence and antibodies

Embryonic and postnatal brain tissue were processed, cryosectioned and immunostained as previously described [10]. Antibodies used were: goat α-GFP (Abcam, ab6673; 1:300), rabbit α-CCND1 (Dako, M3642; 1:300), rabbit α-TBR2 (Abcam, ab23345; 1:300), rat α-phospho-histoneH3 (PH3) (Sigma-Aldrich, H9908; 1:100), rabbit α-SOX2 (Abcam, ab97959; 1:300), rat α-CTIP2 (Abcam, ab18465; 1:300), mouse α-nestin (Abcam, ab6142; 1:100), mouse α-βIII-tubulin (Sigma-Aldrich, T8578), rabbit α-TBR1 (Abcam, ab31940), rabbit α-CUX1 (Santa Cruz Biotechnology, sc-13024), rat α-β1-integrin (Chemicon Millipore, MAB1997). Fluorescent-labelled secondary antibodies were from Jackson ImmunoResearch and were used at 1:300. Images of the staining for further quantification were taken in medial regions around the somatosensory area of the pallium or cortex. RGP length was measured by tracking the process using NeuronJ, a plugin for ImageJ, from the soma of the radial glial cell to the tip of the process. The different embryonic regions of the pallium, including the VZ, SVZ, IZ and the CP, were defined according to differences in nuclear morphology and cell density by DAPI staining.

Immunoblotting

Ccnd1 knock-out protein was extracted from embryo hands in 0.83 M Urea, 0.105 M Tris–HCl pH6.8 and 1.7% SDS, with glass beads in a bead beater homogenizer. To extract protein from rat hippocampal slices, 3–5 slices were collected in 80 ml 1 × SR buffer and homogenized 2 × 10 s with a pellet mixer (VWR®Radnor). Protein concentration was determined by Bradford (BIO-RAD) and finally resuspended in 1x Laemli buffer with 1% b-mercaptoethanol. After 5 min boiling, samples were resolved by SDS-PAGE, transferred to PVDF membranes (Millipore), and incubated with primary antibodies: α-CCND1 (monoclonal DCS-6, BD biosciences, 556470; 1:500), α-CCND1 (polyclonal antibody ABE52, Millipore, 1:1000), α-actin (monoclonal C4, Millipore), α-paxillin (PXN) (monoclonal, BD transduction, 610051, 1:1000), α-pS83 PXN (polyclonal, ECM Biosciences, PP1341, 1:500), α-pS178 PXN (polyclonal, Calbiochem, ST1069, 1:500). Appropriate peroxidase-linked secondary antibodies (GE Healthcare UK Ltd) were detected using the chemiluminescent HRP substrate Immobilon Western (Millipore). Chemiluminescence was recorded with a ChemiDoc-MP imaging system (BioRad).

RNA isolation and real-time quantitative PCR

RNA from cultured cortical neurons collected at different DIV was isolated with RNeasy mini kit (Qiagen), treated with DNAseI (Sigma) and retrotranscribed with SuperScript Reverse Transcriptase (Thermofisher). The obtained cDNA samples were analyzed by Real-time quantitative PCR in a reaction containing 25 ng of cDNA, 1xSYBR Green master mix (Applied Biosystems™ SYBR™, Thermofisher) together with forward and reverse primers (150 nM) for *Ccnd1* (forward 5'-GCGTACCCTGACACCAATCTC-3' and reverse 5'-CTCCTCTTCGCACTTCTGCTC-3') or *Gapdh* as a housekeeping control (forward 5'-AGGTCGGTGTGAACGGATTTG-3' and reverse 5'-TGTAGACCATGTAGTTGAGGTCA-3'). qPCR was performed in the C1000 Thermal Cycler CFX96 Real-Time System (Bio-Rad Laboratories) with the following conditions: initial denaturation at 95ºC for 2 min; 40 cycles at 95ºC for 15 s, 65ºC for 1 min.

Statistical analysis

To evaluate two experimental groups, two-tailed unpaired Student's T test (*t*-Student) was performed. For multiple comparison, one-way ANOVA with a Tukey post-hoc analysis or two-way ANOVA with Sidak's post-hoc analysis was performed. Microsoft Excel and GraphPad Prism v5.0 were used for statistical analysis and graphical representation. The *p* value in each experiment is indicated, and significance was considered when $p<0.05$ (*), $p<0.01$ (**) or $p<0.001$ (***). Error bars were calculated using the standard error of the mean (SEM).

Results

Expression pattern of CCND1 in the developing brain

To understand the function of CCND1 during nervous system development we studied its expression in the brain by immunofluorescence with specific antibodies. As expected, we observed a typical nuclear localization of CCND1 in proliferative regions (VZ and SVZ) alongside the ventricle of embryonic brains, including the pallium, subpallium and thalamus (Fig. 1A). Interestingly, in the E14.5 pallium we noticed that CCND1 displayed a graded expression, from ventro/lateral-high to dorso/medial-low (Fig. 1A, D), that was already visible at E12.5 (Supplementary Fig. 1A)) and that contrasted with the homogenous expression of other proliferation markers such as SOX2 or anti-phospho histoneH3 (PH3) (Fig. 1B, C, E, F) [3]. Surprisingly, CCND1

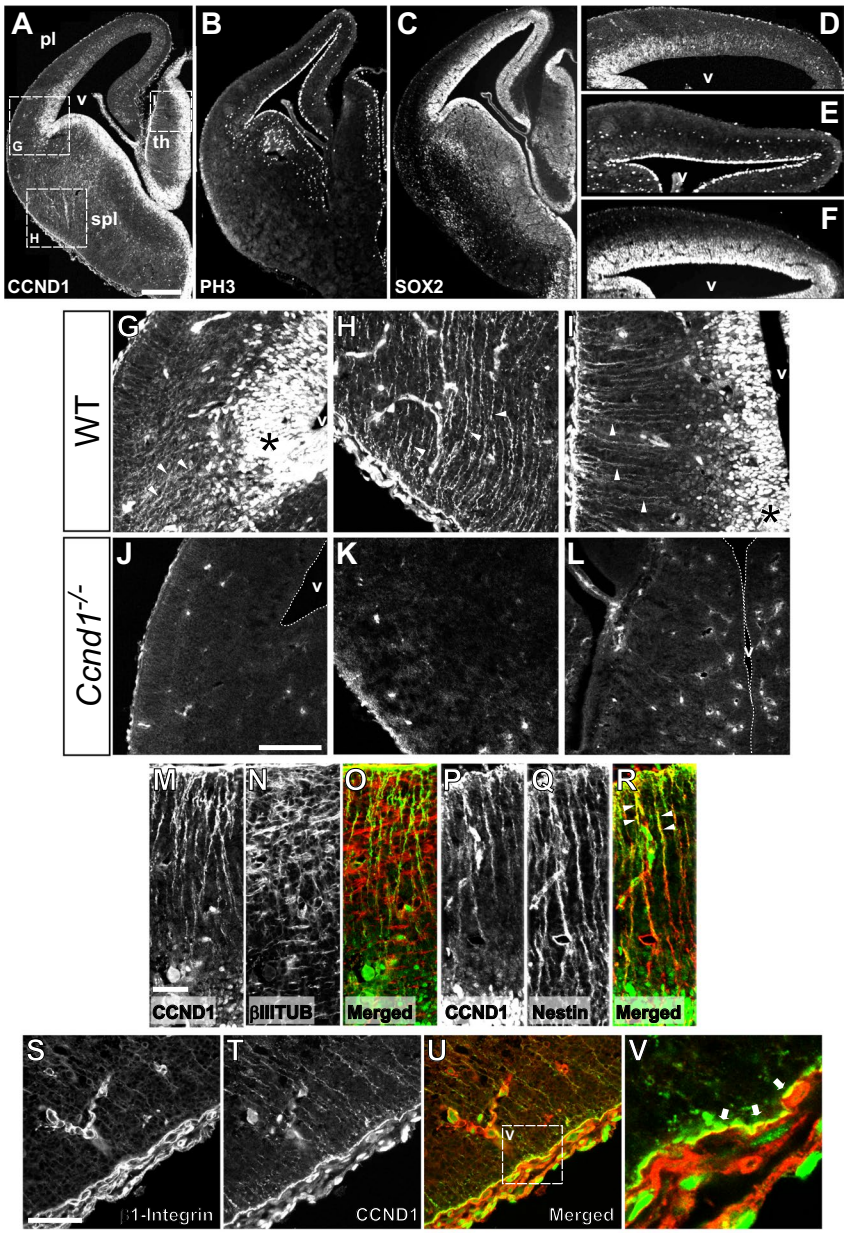

Fig. 1 Expression analysis of CCND1 during brain development reveals a cytoplasmic localization of the protein in the RGPs. **A**-**C**) Images of cryosections of wild-type embryonic brains at E14.5 (only one half of the brain is shown) stained by immunofluorescence with antibodies against CCND1 (A), PH3 (B) or SOX2 (C). Dashed squares in A indicate the position of panels G-I. **D**-**F**) Magnified images of the pallium shown in A-C, stained by immunofluorescence with antibodies against CCND1 (D), PH3 (E) or SOX2 (F). **G**-**I**) Magnified images of the regions shown in A of the pallial-subpallial boundary (G), subpallium (H) or thalamus (I) stained by immunofluorescence with antibodies against CCND1. Asterisks indicate the nuclear staining in the progenitor cell niche. Arrowheads point to the fiber-like staining. **J**-**L**) Images of anti-CCND1 immunofluorescence of the pallial-subpallial boundary (J), subpallium (K) or thalamus (L) on *Ccnd1* knock-out brain sections, at E14.5. **M**-**R**) Images of the thalamus of wild-type embryonic brains at E14.5 stained by immunofluorescence with antibodies against CCND1 (M,P), βIII tubulin (βIIITUB, N), or nestin (Q) and their corresponding merges (O, CCND1 in green; βIII tubulin in red; R, CCND1 in green;nestin in red). The progenitor cell niche is at the bottom of the images. Arrowheads in R point to the co-staining CCND1/nestin at the distal part of RGPs (in yellow). **S**-**V**) Images of the distal end of RGP in the subpallium of wild-type embryonic brains at E14.5, stained by immunofluorescence with antibodies against β1-integrin (S) and CCND1 (T) and the merge (U, CCND1 in green; β1-integrin in red). Dashed square in U indicate the position of panel V. **V**) Magnified image of the region shown in U. Arrows indicate partial overlap of CCND1 and β1-integrin staining (in yellow) at the tip of the RGP. Scale bars: 300 β m (A), 100 β m (J), 50 β m (M,S). Abbreviations: pl, pallium; spl, subpallium; th, thalamus; v, ventricle

staining revealed fiber-like structures in the pallium, thalamus and subpallium indicating a cytoplasmic localization of the protein (Fig. 1A, G, H, I). Nuclear and cytoplasmic CCND1 stainings were specific since both disappeared when *Ccnd1* knock-out tissue was used (Fig. 1J-L). Fiber-like CCND1 localization co-stained with Nestin but not with βIII-tubulin, indicating the presence of cytoplasmic CCND1 specifically in progenitor cells (Fig. 1M-R and data not shown). A closer look at this staining showed that CCND1 localization at the RGP was enriched at the distal, basal end, forming a button-like structure adjacent to the meningeal basement membrane which overlaps partially with the adhesion protein β1-integrin at the plasma membrane (Fig. 1M, P, S-V). In summary, we have described three specific and distinct CCND1 localizations in the mouse developing brain: i) nuclear, in the VZ/SVZ, with a graded pattern from ventro/lateral-high to dorso/medial-low; ii) cytoplasmic at RGPs and iii) at the tip of basal end of the RGP forming a cytoplasmic button-like structure, overlapping with b1-integrin at the plasma membrane, adjacent to the meningeal basement membrane. Association of CCND1 with the plasma membrane was previously reported in non-neuronal cells such as keratinocytes, fibroblasts and cancer cells [9, 12, 13, 53].

Ccnd1 knock-out embryos display normal proliferation but abnormal distribution of TBR2 + and CTIP2 + cells in the developing cortex

We addressed the in vivo relevance of CCND1 during brain development by studying *Ccnd1* knock-out embryos. Given the role of CCND1 in the control of cell cycle, we first assessed proliferation defects in the developing cortex using EdU incorporation or PH3 antibodies. Surprisingly, the distribution and the density of EdU + or PH3 + cells in the pallium from *Ccnd1* knock-out embryos was not affected, indicating that CCND1 is dispensable for proliferation of cortical progenitors (Fig. 2A-F and Supplementary Fig. 1B, C). Next, we studied the structure of the embryonic pallium and postnatal cortex of these animals with several markers including TBR2, which labels intermediate progenitor cells in the SVZ during development, or CUX1, CTIP2 and TBR1, which label different layers of the mature cortex. At embryonic stages 16.5 and 18.5 (E16.5 and E18.5), we found that *Ccnd1* knock-outs exhibited TBR2 + cells scattered in upper cortical positions, outside of the SVZ (Fig. 2G-L), without changing the total amount of TBR2 + cells (Supplementary Fig. 1D). Likewise, at postnatal stage 8 (P8), we observed that some CTIP2 + neurons, which in control animals are restricted to cortical layer V, were ectopically located in upper and deeper positions (Fig. 2M-O). However, the distribution of CUX1 (upper-layers II-III) and TBR1 (inner layer VI) was unaltered (Supplementary Fig. 1E-J). Altogether, these results indicate that CCND1 is required for proper cortical layering, mainly affecting layer V neurons, independently of its role on cell proliferation, and therefore suggest a different mechanism of action of CCND1 during brain development.

Neurons expressing a cytoplasmic dominant negative CCND1 ($CCND1^{CAAXK112E}$) reproduce some of the layering defects observed in the *Ccnd1* knock-out embryos

We and others have reported additional functions of CCND1 besides cell cycle control, including the regulation of cytoplasmic targets [12, 23, 53]. Since CCND1 in the RGC process was observed adjacent to the plasma membrane, overlapping with b1-integrin, we investigated if in this localization CCND1 had a specific role during cortex development. For that we constructed a version of the protein with a preferred localization in cytoplasmic membranes. This was achieved by adding the CAAX box of KRas, including a polybasic domain adjacent to the CAAX motif, to the C-terminus of CCND1 ($CCND1^{CAAX}$) that allows its prenylation and tethering mainly to the plasma membrane [14, 20]. We have previously validated this mutant and observed

Fig. 2 *Ccnd1* knock-out animals display cortical layering abnormalities but not proliferation defects. **A** and **B**) Representative images of EDU fluorescent staining on cortical sections from wild-type (WT) or *Ccnd1* knock-out embryos (E14.5), obtained from pregnant females injected for 1 h with EDU. The 10 bin division of the cortical wall used for quantification is indicated on the right and the SVZ on the left. **C**) Quantification of the percentage of EDU + cells in each bin along the cortical wall of the sections shown in A,B (black bars, WT; white bars, *Ccnd1* knock-out). Values are expressed as mean ± SEM ($n = 3$ embryos; > 3 sections/embryo; > 100 cells/section). No statistical differences were observed (two-way ANOVA). **D**) Comparison of the density of EDU + cells in cortical sections (E14.5) from wild-type (WT, black bar) or *Ccnd1* knock-out embryos (KO, white bar). Values are expressed as mean ± SEM ($n = 3$ embryos; > 3 sections/embryo; > 100 cells/section). No statistical differences were observed (*t*-Student). **E**) Quantification of the percentage of PH3 + cells in each bin along the cortical wall of the sections stained with anti-PH3 antibodies (black bars, WT; white bars, *Ccnd1* knock-out). Values are expressed as mean ± SEM ($n = 3$ embryos; > 6 sections/embryo; > 20 cells/section). No statistical differences were observed (two-way ANOVA). **F**) Comparison of the density of PH3 + cells in cortical sections (E14.5) from wild-type (WT, black bar) or *Ccnd1* knock-out embryos (KO, white bar). Values are expressed as mean ± SEM ($n = 3$ embryos; > 6 sections/embryo; > 20 cells/section). No statistical differences were observed (*t*-Student). **G-J**) Representative images of cortical sections from wild-type (WT) or *Ccnd1* knock-out embryos at E16.5 (G,H) or E18.5 (I,J) stained with TBR2 antibodies. The 10 bin division of the cortical wall used for quantification is indicated on the right and the SVZ on the left. Arrowheads in H and J point to TBR2 + cells outside the SVZ. Asterisk in H indicates non-specific signal from the staining. **K**, **L**) Quantification of the percentage of TBR2 + cells in each bin along the cortical wall of sections stained in G-J, as indicated (black bars, WT; white bars, *Ccnd1* knock-out). Values are expressed as mean ± SEM ($n = 4$ embryos; > 5 sections/embryo; > 30 cells/slide). Significance was determined by two-way ANOVA and Sidak's multiple comparison (*$p < 0.05$;**$p < 0.01$). **M** and **N**) Representative images of cortical sections from wild-type (WT) or *Ccnd1* knock-out postnatal brains (P8), stained with anti-CTIP2 antibodies. The 10 bin division of the cortical wall used for quantification is indicated on the right. **O**) Quantification of the percentage of CTIP2 + cells in each bin along the cortical wall of sections stained in M,N (black bars, WT; white bars, *Ccnd1* knock-out). Values are expressed as mean ± SEM ($n = 3$ animals; > 3 sections/animal). Significance was determined by two-way ANOVA and Sidak's multiple comparison (**$p < 0.01$). Scale bar: 100 µm

that $CCND1^{CAAX}$ was mostly localized at the plasma membrane and cytoplasm and was barely present in the nucleus [13]. Similarly, in dissociated cortical neurons, transfected $CCND1^{CAAX}$ shows a cytoplasmic expression, fulfilling the neuron processes and excluding the nucleus (see Supplementary Fig. 2L). $CCND1^{CAAX}$ was then subcloned into the pCAGIG vector that contains an IRES EGFP reporter gene for tracking of the electroporated cells and for visualization of their morphology during in utero electroporation (IUE) experiments. As a control we used the empty vector (pCAGIGempty). In addition, we included a cytoplasmic-specific dominant negative CCND1 ($CCNDd1^{CAAXK112E}$), in which the lysine 112 (K112) was substituted by a glutamic acid (E) rendering a protein that while still binding CDKs is unable to trigger their kinase activity [25]. All these constructs were IUE at E13.5 and the structure and laminar organization of

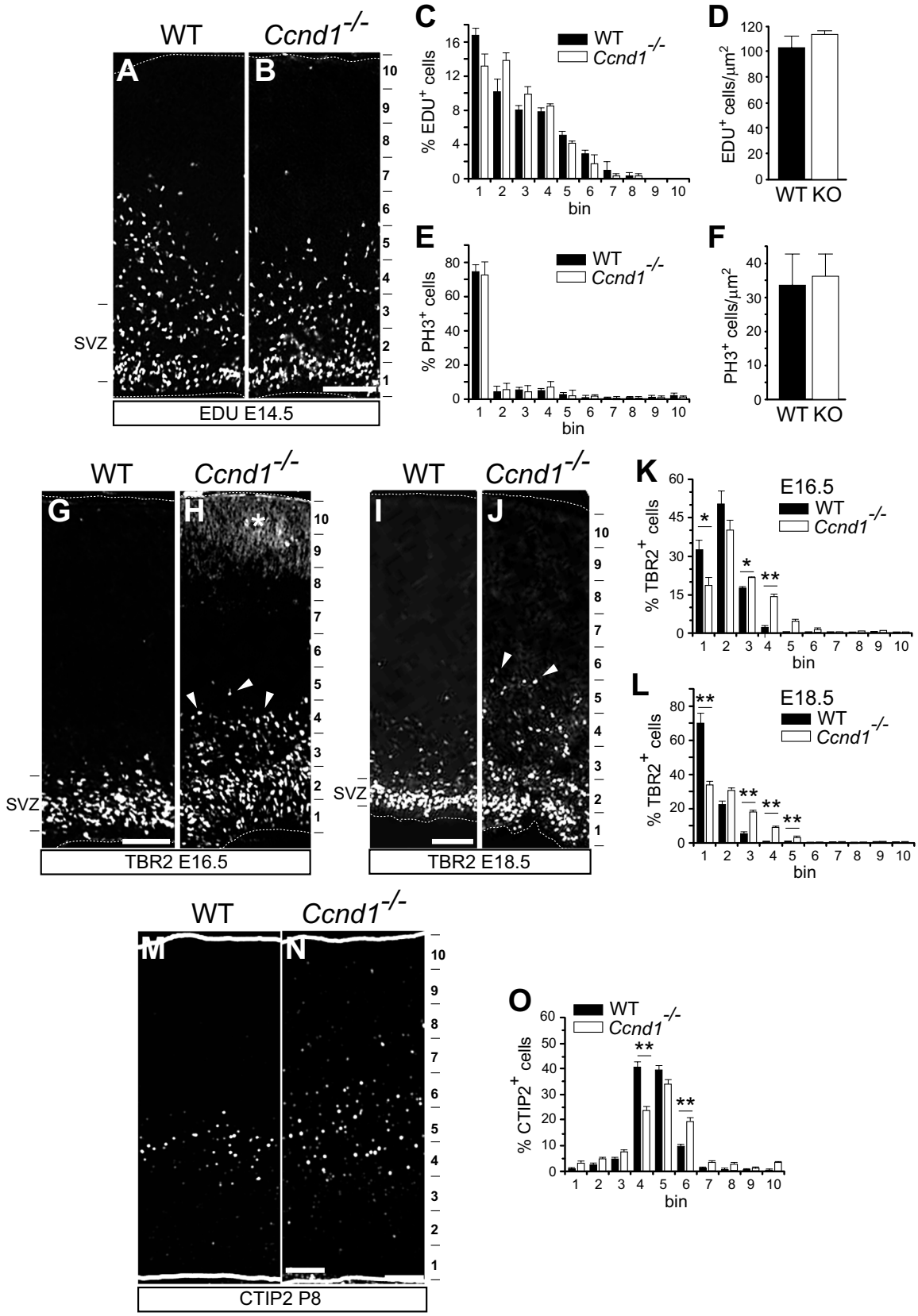
WT
Ccnd1-/-
A
B
SVZ
EDU E14.5
C
% EDU+ cells
bin
D
EDU+ cells/μm2
WT KO
E
% PH3+ cells
F
PH3+ cells/μm2
G
H
I
J
TBR2 E16.5
TBR2 E18.5
K
E16.5
% TBR2+ cells
L
E18.5
M
N
CTIP2 P8
O
% CTIP2+ cells

the pallium/cortex was studied few days later during embryonic and postnatal stages. None of these constructs induced cell death (data not shown). At E16.5, electroporation of CCND1^{CAAX} or CCND1^{CAAXK112E} resulted in an increase of EGFP+cells in upper parts of the pallium when compared to the empty vector control (Fig. 3A, E, I, M). Then, we studied the distribution of the TBR2+;EGFP+double positive cells. In empty vector control and CCND1^{CAAX} electroporated brains the percentage of TBR2+;EGFP+outside the SVZ among the total EGFP+cells was very low, and no differences were observed between these two conditions (Fig. 3A-H, N). In contrast, electroporation of the dominant negative CCND1^{CAAXK112E} triggered a massive increase of TBR2+;EGFP+cells outside the SVZ, including

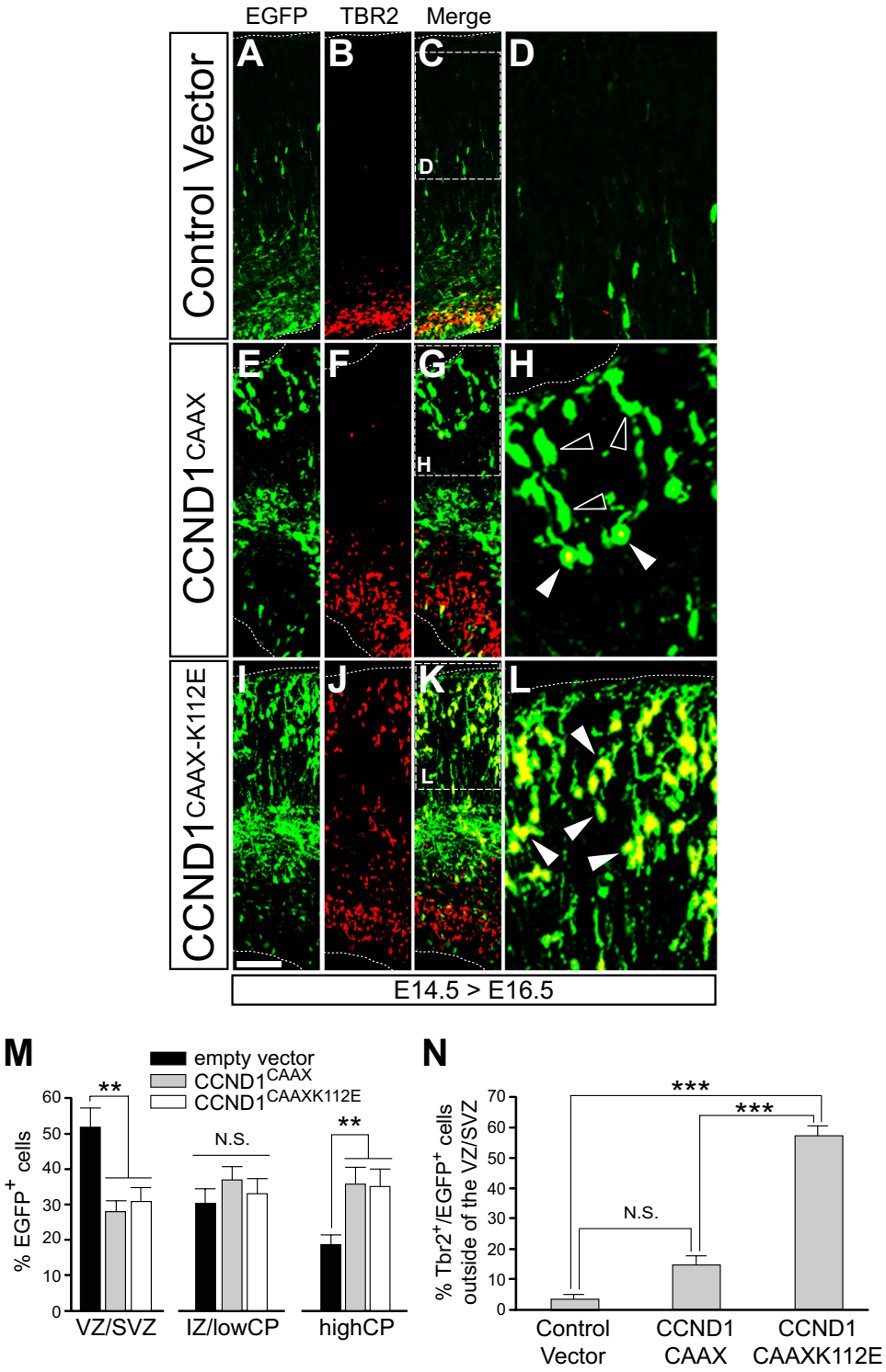

Fig. 3 Expression of CCND1^{CAAXK112E} affects the distribution of TBR2+cells in the developing cortex. Wild-type embryos were IUE at E14.5 with the indicated constructs in pCAGIG vector, and fixed at E16.5: empty vector (A-D), CCND1^{CAAX} (E–H) or CCND1^{CAAXK112E} (I-L). **A-C**, **E–G**, **I-K**) Overview images of the electroporated pallium with the indicated constructs stained by immunofluorescence with antibodies against EGFP (A,E,I) or TBR2 (B,F,J). Merged images are shown in C,G,K (EGFP in green; TBR2 in red). Dashed squares in C, G and K indicate the position of panels D, H and L, respectively. **D**, **H**, **L**) Magnified images of the CP indicated in C,G,K of the merged EGFP/TBR2 double staining. Empty arrowheads point to EGFP-only stained cells; solid arrowheads point to cells displaying both markers. M) Quantification of the percentage of EGFP+cells along the cortical wall divided in three regions VZ/SVZ, IZ/lowCP and highCP of embryos IUE with empty vector (black bars), CCND1^{CAAX} (grey bars) or CCND1^{CAAXK112E} (white bars) at E13.5 and fixed at E16.5. Values are expressed as mean±SEM ($n=4$ embryos; >3 sections/embryo). Significance in each region was determined by one-way ANOVA and Tukey-HSD post-hoc test (**$p<0.01$; N.S., non-statistically significant difference).N) Quantification of the percentage of double EGFP/TBR+cells outside of the VZ/SVZ among the total EGFP+cells in the pallium of the electroporated embryos with the indicated plasmids. Values are expressed as mean±SEM (n>5 sections from>3 electroporated embryos; >30 cells/section). Significance was determined by one-way ANOVA and Tukey-HSD post-hoc test (***$p<0.001$; N.S., non-statistically significant difference). Scale bar: 100 µm

the intermediate zone (IZ) and upper regions of the CP (Fig. 3I-L, N). These ectopic EGFP+cells were negative for proliferation markers such as PH3, indicating that they are not proliferating cells (Supplementary Fig. 1K-M). These results suggest that the cytoplasmic fraction of CCND1 is required for the proper layering of the pallium. Next, we studied the distribution of CTIP2+cells at P8 in CCND-1^{CAAXK112E} electroporated brains. As in E16.5, the distribution of EGFP cells shifted towards the upper part of the pallium when compared to the empty vector control (Fig. 4A, B, H, I). In addition, we noticed a significant increase of CTIP2+cells in upper bins of these brains, outside of its normal localization at this stage in layer V (Fig. 4C,D,K,L) and a significant increase of both EGFP+;CTIP2+cells in this area (Fig. 4M). This was not an effect of ectopic CTIP2 expression due to CCND1^{CAAXK112E} electroporation, as the total amount of CTIP2+cells was not increased but, indeed, slightly decreased (Fig. 4J). Of note, not all the CTIP2+cells in these upper bins seem positive for EGFP, suggesting either a low EGFP signal in these cells or a non-cell autonomous effect of the dominant negative CCND-1^{CAAXK112E} (Fig. 4E-G). The observation of TBR2+and CTIP2+cells above their normal localization when electroporating CCND1^{CAAXK112E} is partially reminiscent of the abnormal distribution of these two cell populations in the *Ccnd1* knock-out brains (Fig. 2). However, in the case of CCND1^{CAAXK112E}, the TBR2+cells found within the CP at E16.5 and the CTIP2+cells found in upper bins at P8, were not observed in the *Ccnd1* knock-out mutants. This suggests that perhaps its dominant negative effect sequesters more CDK effectors than those affected by *Ccnd1* deletion, causing a stronger effect. In conclusion, our results indicate that cytoplasmic CCND1 plays an important role during cortex development and layer organization.

Cytoplasmic, membrane-associated, CCND1 affects the morphology of progenitor cells and of migrating neurons and affects cortical neuron distribution

To understand the cellular base of these layering defects, we first performed shorter IUE time experiments in which embryos were collected 12 h after electroporation at E13.5. As expected, after 12 h most of the electroporated cells with pCAGIGempty were progenitors within the VZ/SVZ, with many RGPs extending towards the basal surface (Fig. 5A, D). In contrast, very few and shorter RGPs were observed when CCDN1^{CAAX} was electroporated (Fig. 5B, D). On the other hand, brains electroporated with the dominant negative CCND1^{CAAXK112E} displayed longer RGPs and a higher proportion of RGPs bound to the meningeal basement membrane than empty vector control (Fig. 5C-E) even 24 h after electroporation (Supplementary Fig. 1N-T). These CCND1^{CAAXK112E} processes were positive for nestin, indicating that they were indeed RGPs (Supplementary Fig. 1P-R). Since the electroporation time was short, we assumed that CCND1^{CAAX} accelerated the retraction of the preexisting RGP while CCND1^{CAAXK112E} slowed this process, indicating that proper detachment of the RGP from the meningeal basement membrane during cortex development requires membrane-associated cytoplasmic CCND1/CDK activity. Three days after electroporation (E16.5) we observed that the cells found in the high CP adopted different morphologies and they were multipolar, unipolar/bipolar or were attached to the basement membrane (ABM). In the empty vector control condition, most cells in the high CP displayed unipolar/bipolar morphology or were ABM (Fig. 5F, I-K). However, CCND1^{CAAX} expressing cells displayed a robust increase of multipolar cells in the CP compared to cells electroporated with the empty vector control or with the CCND1^{CAAXK112E} (Fig. 5G, I-K). By contrast, electroporation with CCND1^{CAAXK112E} showed a significant increase of ABM cells in the CP (Fig. 5H, I-K). In summary, these results demonstrate that changes of cytoplasmic, membrane-bound, CCND1 expression modulate the morphology of the RGP of progenitor cells and migrating neurons in vivo, during cortex development through CDK activity.

Cytoplasmic CCND1 promotes neurite and axon outgrowth and increases neurite number in primary cortical neurons

In order to assess more in detail the morphological effects of cytoplasmic CCND1 observed in vivo by IUE, we used dissociated cortical neurons from embryonic mouse brains. This is not a perfect model because neurons become rapidly postmitotic in culture as evidenced by the fast decline of *Ccnd1* expression, being almost undetectable after 3-4DIV (Supplementary Fig. 2A). In fact, experimental re-expression of wild-type CCND1 induced cell death (Supplementary Fig. 2B-F), an effect that has been widely reported in neurons [49]. Therefore, we performed these experiments within this 3-4DIV-time window, and we chose the electroporation as transfection method to quickly induce gene expression. We then co-transfected these neurons with CCND1^{CAAX} or CCND1^{CAAXK112E} together with a plasmid encoding EGFP, as a reporter. Interestingly, overexpression of any of the two cytoplasmic, membrane-bound, CCND1 constructs did not trigger cell death, and the cultures were viable after 4DIV (Supplementary Fig. 2G-K). Instead, CCND1^{CAAX} significantly increased the length of the main axon, the total length of neurites and the number of neurites per cell compared to the empty vector control (Fig. 6A, B, D, F–H). These effects were not observed in

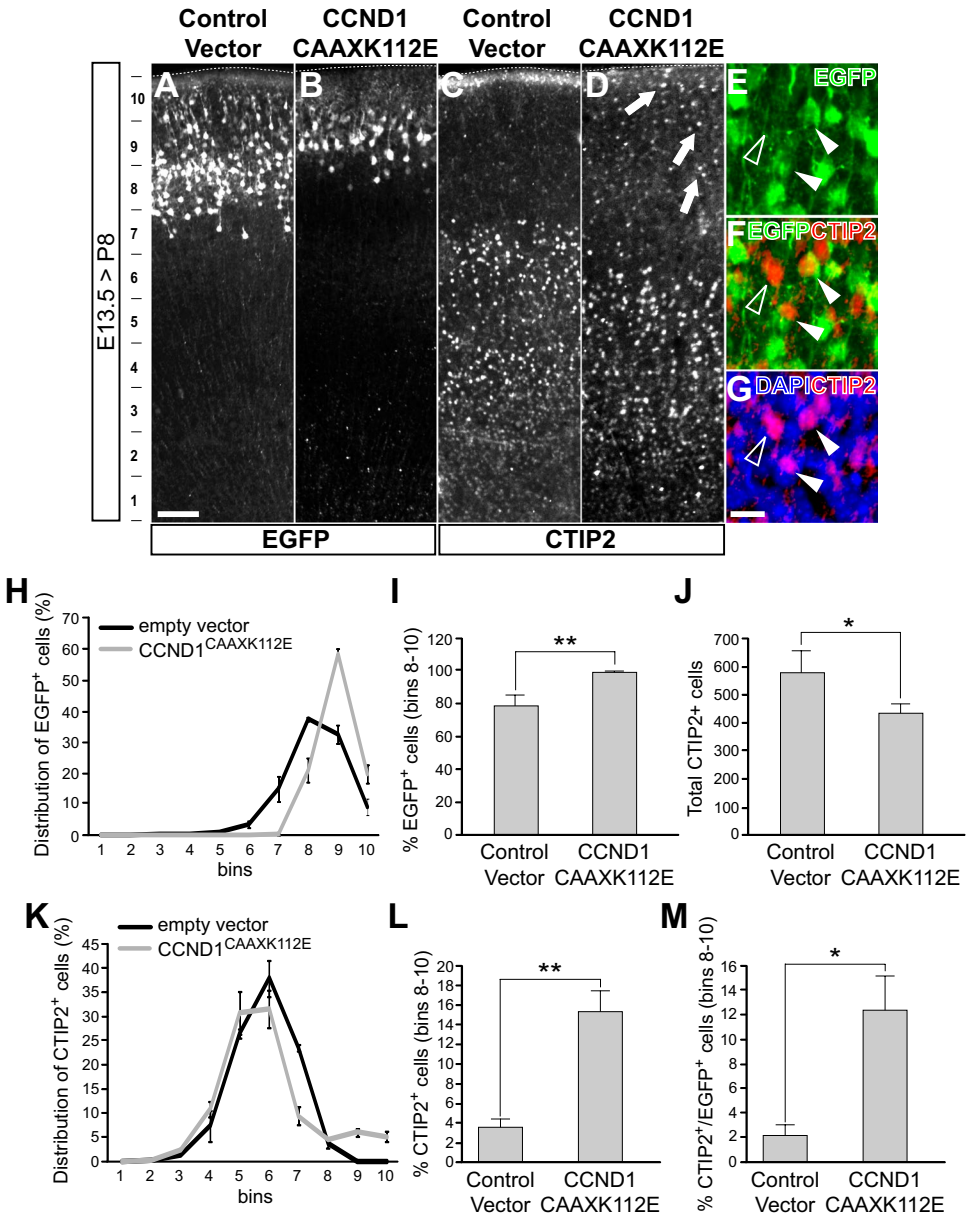

Fig. 4 Expression of CCND1^{CAAXK112E} affects the distribution of CTIP2+cells in the postnatal cortex. Wild-type embryos were IUE at E13.5 with the indicated constructs in pCAGIG vector, and fixed at P8: empty vector (A,C) or CCND1^{CAAXK112E} (B,D). **A-D**) Overview images of the electroporated cortex with the indicated constructs stained by immunofluorescence with antibodies against EGFP (A,B) or Ctip2 (C,D). Arrows in D point to CTIP2+cells in upper bins. The bins used to quantify the positive cells are shown to the left of panel A. **E**–**G**) Representative magnified images of the upper bins area of CCND1^{CAAXK112E} electroporated brains merging the EGFP in green, CTIP2 in red and DAPI in blue, as indicated. Empty arrowheads point to CTIP2-only stained cells; solid arrowheads point to cells displaying both EGFP and CTIP2 markers. **H**) Distribution of the percentage of EGFP+cells along the cortex width divided into 10 equal bins as indicated in A for both empty vector control (black line) or CCND1^{CAAXK112E} (grey line) IUE brains (n≥3 embryos; >5 sections/embryo). **I**) Percentage of EGFP+cells in upper bins (8–10) in empty vector or CCND1^{CAAXK112E} IUE brains, as indicated. Values are expressed as mean±SEM (n≥3 embryos; >5 sections/embryo). Significance was determined by *t*-Student (**$p<0.01$).J) Total number of CTIP2+cells in empty vector or CCND1^{CAAXK112E} IUE brain sections, as indicated. Values are expressed as mean±SEM (n≥3 embryos; >5 sections/embryo). Significance was determined by *t*-Student (*$p<0.05$). **K**) Distribution of the percentage of CTIP2+cells along the cortex width divided into 10 equal bins as indicated in A for both empty vector control (black line) or CCND1^{CAAXK112E} (grey line) IUE brains (n≥3 embryos; >5 sections/embryo). **L**) Percentage of CTIP2+cells in upper bins (8–10) in empty vector or CCND1^{CAAXK112E} IUE brains, as indicated. Values are expressed as mean±SEM (n≥3 embryos; >5 sections/embryo). Significance was determined by *t*-Student (**$p<0.01$). **M**) Percentage of double EGFP+;CTIP2+cells out of total EGFP+cells in upper bins (8–10) in empty vector or CCND1.^{CAAXK112E} IUE brains, as indicated. Values are expressed as mean±SEM ($n≥3$ embryos; >5 sections/embryo). Significance was determined by *t*-Student (*$p<0.05$). Scale bars: 20 µm (G), 100 µm (A)

cultures transfected with CCND1^{CAAXK112E} indicating that CDK activity is necessary (Fig. 6C, E, F–H). Consistent with these observations, the transfection of a membrane-targeted CDK4 (CDK4^{CAAX}) was sufficient to trigger similar morphological changes (Supplementary Fig. 2M, N). In addition, we performed loss-of-function experiments to address the role of CCND1 in neuron morphology at 1DIV. First, we transfected neurons with a specific *Ccnd1* shRNA (Supplementary Fig. 2O) and observed the opposite effect to CCND1^{CAAX} overexpression, i.e. significant reductions of axon and neurite lengths, and of the number of neurites per cell compared to a scramble control (Fig. 6I-K). Second, we used cultures from *Ccnd1* knock-out embryos and observed similar results as in the knock-down approach, a significant reduction of axon and neurite length compared to control littermates (Supplementary Fig. 2P-R). Altogether, these results reveal that CCND1 modulates neuron morphology in vitro and that the cytoplasmic, membrane-bound, fraction of the protein, through the activation of CDKs, is the major effector of this function. The increase in neurite number due to cytoplasmic CCND1 expression in neurons in vitro could explain the increase in multipolar neurons observed in the CP, induced by CCND1^{CAAX} expression, in vivo.

Cytoplasmic effects of CCND1 are mediated by the integrin signaling complex effector paxillin

We have previously shown that CCND1 associates with paxillin at the plasma membrane and regulates fibroblast and tumor cell migration and cell–matrix adhesion through CDK4 and the phosphorylation of paxillin, a member of the signaling complex of integrins in focal adhesions [12]. We characterized the serine residues 83 and 178 as the major phosphorylation sites of CCND1/CDK complexes [12]. We therefore addressed the possibility that paxillin mediates the cytoplasmic effects of CCND1 in neurons at the plasma membrane. First, we observed that paxillin phosphorylation at S83 and S178 rapidly decreased in culture (Fig. 7A-C). Interestingly, this response correlated with the reduction of CCND1 levels (Supplementary Fig. 2A), suggesting that paxillin might be a target of CCND1/CDK complexes also in neurons. This was confirmed by using palbociclib, a CDK4/6 specific inhibitor, which completely abolished paxillin phosphorylation at S83 in slices of rat hippocampi (Fig. 7D). To interfere with the CCND1/CDK-dependent paxillin phosphorylation within the cells we used a phosphorylation mutant where the two serine residues 83 and 178 targeted by CCND1/CDKs were substituted by alanine residues (paxillin$^{S83A;S178A}$; [12]). When this mutant was transfected in cortical neurons, both neurite and axon length were significantly reduced (Fig. 7E, F). This effect was similar to that observed using *Ccnd1* knock-out or knock-down cultures (Fig. 6I-K and Supplementary Fig. 2Q-R) and the opposite of cytoplasmic CCND1 overexpression (Fig. 6F-H). Altogether, these results are consistent with paxillin being an important effector of membrane-associated CCND1/CDK complexes for controlling neuron morphology, in vitro. We finally addressed if paxillin phosphorylation by CCND1/CDKs could also be relevant in vivo during nervous system development. For this, we IUE paxillin$^{S83A;S178A}$ in cortical progenitors of wild-type embryos at E13.5 and compared the morphology of the electroporated cells with empty vector or wild-type paxillin, 12 h later. This short time was selected to visualize exclusively the preexisting RGPs. We observed that wild-type paxillin caused a significant detachment and retraction of the RGPs from the meningeal basement membrane as the number of RGPs attached to the basement membrane and their length was dramatically reduced compared to empty vector control (Fig. 7G-I). This effect was not observed when paxillin$^{S83A;S178A}$ was electroporated (Fig. 7G-I). Instead, compared to empty vector control, paxillin$^{S83A;S178A}$ displayed an increase of the number of RGPs bound to the meningeal basement membrane (although not statistically significant) and a significant increase of RGP length (Fig. 7H, I). Taking into consideration these observations and the results from Fig. 5A-D, we conclude that both CCND1 and paxillin are required for the correct detachment of the RGP from the basement membrane, in vivo. Although our experiments cannot rule out the participation of CCND2 in paxillin phosphorylation in this context, we believe that CCND1 is primarily involved. This is supported by the observation that, at the time where our IUE experiments with paxillin were performed, CCND1 is mainly expressed in the VZ and SVZ whereas CCND2 expression is found in the SVZ but absent from the VZ [15]. Therefore, we propose that CCND1 and paxillin are part of the same signaling pathway in which CCND1/CDK complex would phosphorylate paxillin at the plasma membrane and control RGP adhesion to the meningeal basement membrane.

Discussion

During nervous system development, the molecular mechanisms controlling proliferation are tightly regulated to achieve the correct timing for neuron differentiation. In the present work we have shown that CCND1 plays key functions during cortex development independent of its well-established role on cell cycle regulation. Instead, we have shown that CCND1 is also localized in the cytoplasm and associated to the plasma membrane of the RGPs of cortical neuron progenitors. Our results suggest that in this localization CCND1 regulates meningeal basement membrane

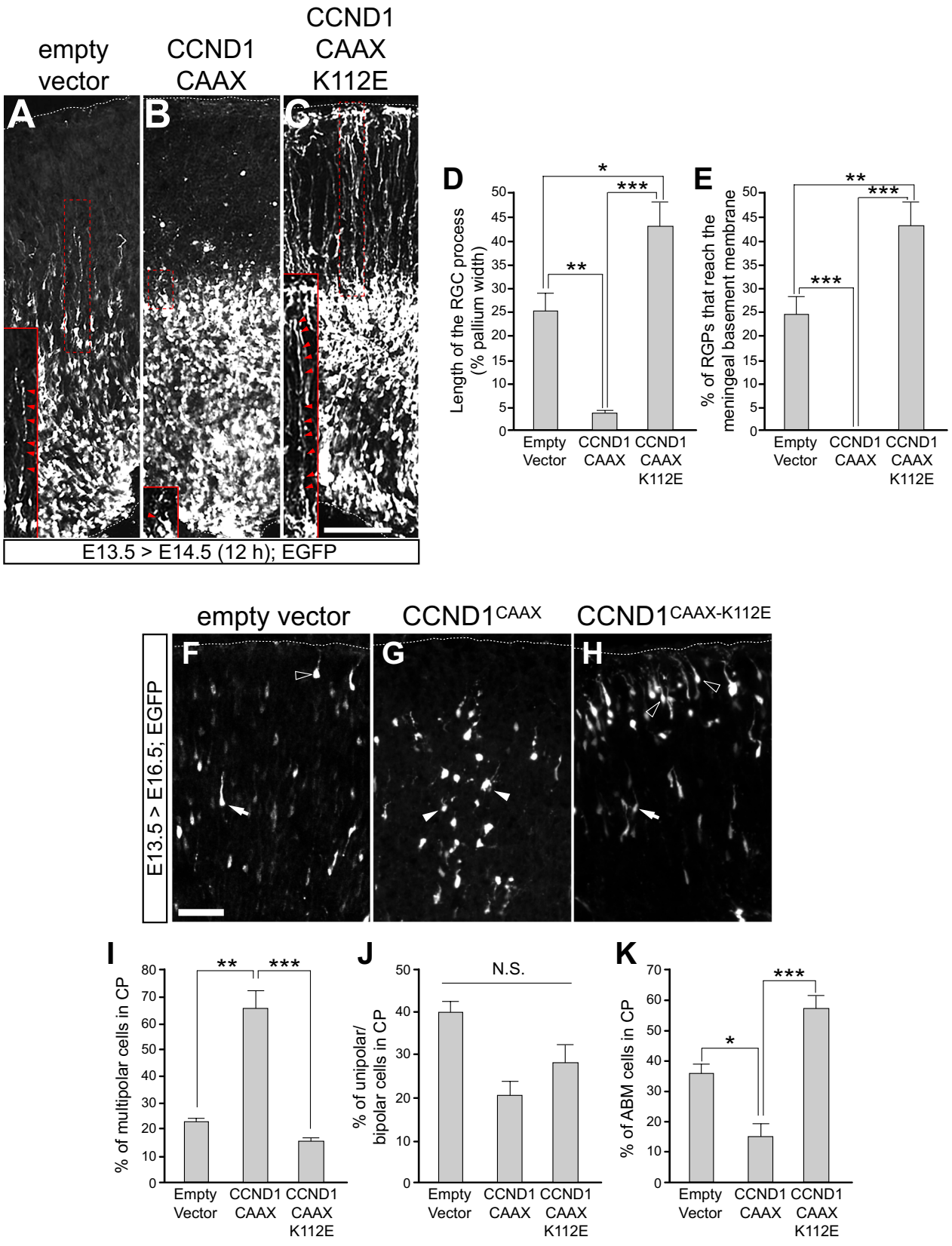
empty vector
CCND1 CAAX
CCND1 CAAX K112E
A
B
C
E13.5 > E14.5 (12 h); EGFP
D
Length of the RGC process (% pallium width)
Empty Vector
CCND1 CAAX
CCND1 CAAX K112E
E
% of RGPs that reach the meningeal basement membrane
empty vector
CCND1CAAX
CCND1CAAX-K112E
E13.5 > E16.5; EGFP
F
G
H
I
% of multipolar cells in CP
J
% of unipolar/ bipolar cells in CP
N.S.
K
% of ABM cells in CP

Fig. 5 Cytoplasmic CCND1 affects RGP and neuron morphology in vivo. **A-C**) Representative images of cortical sections from wild-type mouse embryos IUE with the indicated constructs in pCAGIG vector at E13.5 and analyzed 12 h later. The brains were dissected, fixed and analyzed by immunofluorescence with an anti-EGFP specific antibody. Insets show a representative RGP (indicated with a dashed box) in each condition and arrowheads illustrate the trajectory of the RGP considered for the quantification. Scale bar: 100 µm. **D** and **E**) Quantification of the relative length of the RGP to the pallium width (D) or the percentage of RGP attached to the meningeal basement membrane (E) of the experiment shown in A-C. Values are expressed as mean ± SEM ($n = 4$ embryos; > 20 processes per experimental condition for each embryo). Significance was determined by one-way ANOVA and Tukey-HSD post-hoc test (*$p < 0.05$;**$p < 0.01$;***$p < 0.001$). **F**–**H**) Representative images of the highCP region showing the morphology of the EGFP + IUE at E13.5 with the indicated plasmids and analyzed at E16.5. Arrows indicate unipolar/bipolar cells, filled arrowheads indicate multipolar cells and empty arrowheads indicate cells attached to the basement membrane (ABM). Scale bar: 50 mm. **I-K**) Quantification of the different cell morphologies of the EGFP + cells found in the highCP: multipolar (I), unipolar/bipolar (J) or attached to the basement membrane (ABM, K) of embryos IUE with the indicated vectors at E13.5 and fixed at E16.5. Values are expressed as mean ± SEM ($n > 4$ sections from 3 electroporated embryos, 20–120 cells per section). Significance in each region was determined by one-way ANOVA and Tukey-HSD post-hoc test (*$p < 0.05$;**$p < 0.01$;***$p < 0.001$; N.S., non-statistically significant difference)

adhesion through paxillin, a downstream effector of integrins in focal adhesions. Moreover, we show that alteration of cytoplasmic CCND1 levels affect cortical layering and neuron morphology in vivo and in vitro. A summary of our results is shown in Fig. 7J.

As it was reported previously, we found that the brain of *Ccnd1* knock-out animals developed normally, without gross morphological defects and no alteration of specific proliferation markers [16]. In fact, just mild proliferation defects were described at P0 in the granule progenitor cells leading to a reduction of postnatal cerebellar size [40]. *Ccnd2* seems to have a more prominent role in the proliferation of cortical precursors in vivo as its genetic ablation causes G1 lengthening, premature cell cycle exit and faster neuronal differentiation, leading to microcephaly and thinner cortical wall [16]. Indeed, genetic variants of the *CCND2* gene in humans have been described that produce a gain-offunction protein and that have been associated to polymicrogyria and megalencephaly [21, 32] while loss of function variants have been linked to microcephaly [39].

The *Ccnd1* loss-of-function data contrasts with the effects of CCND1 overexpression in cortical progenitors. Electroporation of CCND1/CDK4, CCND1 or CCNE1 shortens G1, promoting the expansion of progenitor cells and delaying neurogenesis [26, 38]. Similar results were observed in neural stem cells of the adult hippocampus and olfactory bulb [1, 4]. Previous studies have suggested redundant functionality among CCNDs, in vivo [6, 24, 43]. Both CCND2 and CCND1 display partial overlapping expression in the developing cortex and CCND2 can indeed replace the function of CCND1 in cortical proliferation [15, 16].

Besides cell cycle control, CCND1 exhibits additional functions in multiple tissues and cell types suggesting a more intricate mechanism of action [23]. For instance, in granule progenitor cells, CCND1/CDK4 complex phosphorylates the transcription factor ATOH1, preventing its degradation, which is essential for maintaining their immature state [11, 33]. By contrast, in cortical neuron progenitors CCND1 promotes lineage-commitment and differentiation while CCNB1/2 favour self-renewal of radial glial cells [18]. In line with this last study, we show a graded expression of CCND1 in the developing cortex, from ventro/lateral-high to dorso/medial-low, which has been reported to be controlled by the transcription factor SP8 and related to neuronal differentiation [3]. Pro-neurogenic functions of CCND1 were previously reported. For example, CCND1 expression, but not CCND2, is maintained during the initial phase of motoneuron differentiation and stimulates neurogenesis by a cell cycle-independent mechanism involving the pro-neurogenic transcription factor Hes6 [29]. In addition, in PC12 cells the neurotrophic factor NGF activates CCND1 expression, which is necessary for neurite outgrowth [30]. Consistently, we show that ablation or downregulation of *Ccnd1* in mouse cortical neurons cause a significant reduction of neurite complexity. This could be explained by the regulation of pro-neurogenic transcription factors by CCND1 [29]. However, our results point to an alternative, not mutually exclusive, interpretation. We suggest that cytoplasmic, membrane associated, CCND1 is required for neuron differentiation as the overexpression of $CCND1^{CAAX}$ enhances neuron complexity while $CCND1^{CAAXK112E}$ has no effect, indicating the requirement of CDK activity in this effect. Thus, we provide a novel cell cycle-independent function of CCND1/CDK complex that requires cytoplasmic localization.

Cytoplasmic localization of CCND1 in postmitotic hippocampal and cortical neurons and neuroblastoma cells was previously observed. This was first proposed as a mechanism to prevent apoptosis and/or for cell cycle withdrawal [44, 48, 49]. However, we and others have provided evidence in cancer cells and embryonic fibroblasts that cytoplasmic CCND1 can be found as well associated to the plasma membrane and has an active role in controlling cell adhesion or motility with different intracellular mechanisms involved (see below). In the context of neuronal function, it was recently reported that extracellular vesicles from NGF-differentiated PC12 cells contain CCND1, which is necessary to induce neuronal lineage of stem cells [47]. In addition, we have shown that cytoplasmic CCND1/CDK complex controls postmitotic neuronal communication by phosphorylation of the α4 subunit of GABAA receptors [37].

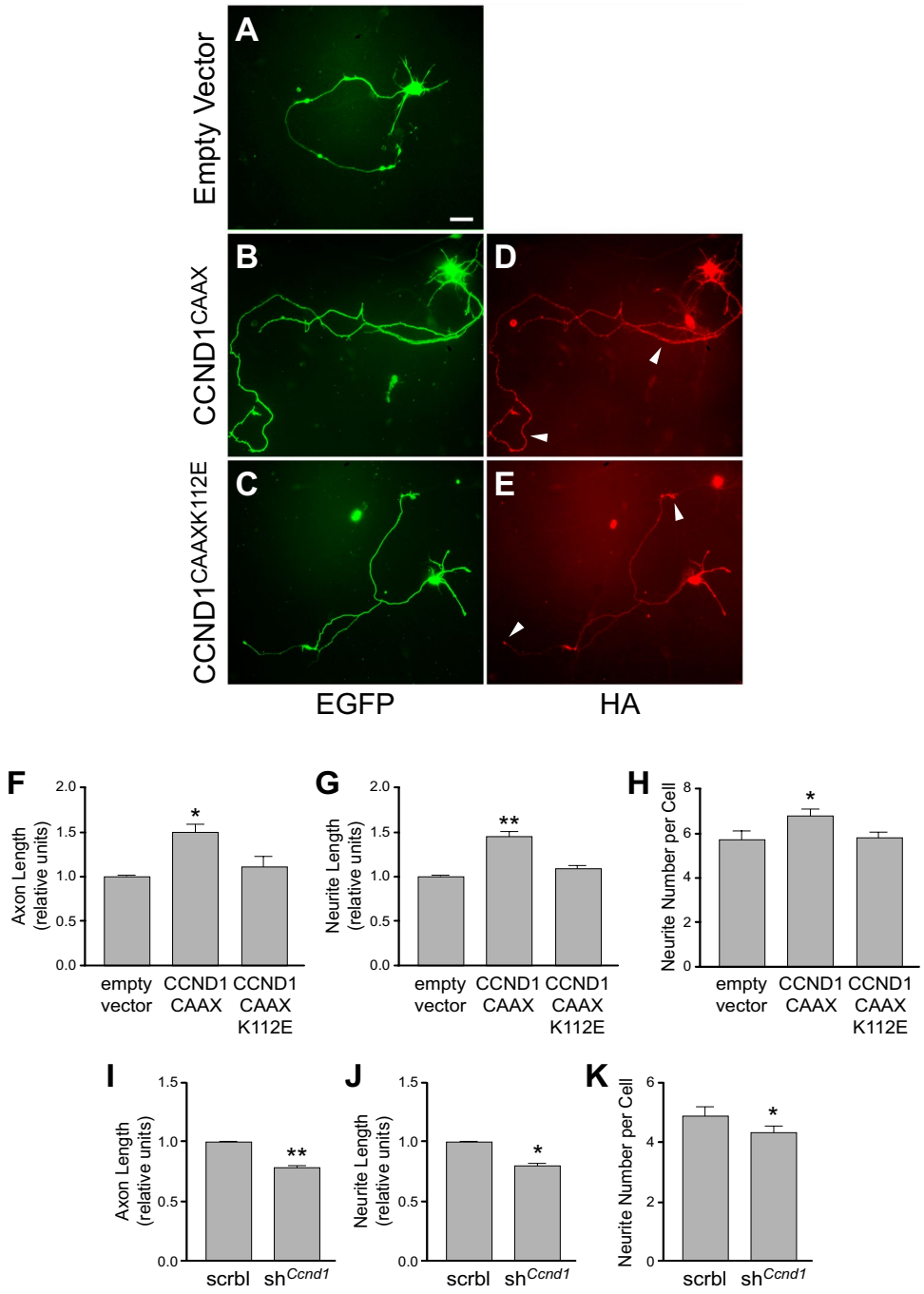

Fig. 6 Cytoplasmic CCND1 affects neuron morphology in vitro in a CDK-dependent manner. **A**-**E**) Representative images of mouse cortical neuron cultures co-electroporated before seeding with the indicated constructs with an HA tag in pcDNA3 (empty vector as a negative control), and a plasmid encoding EGFP. After 4DIV, cultures were fixed and analyzed by immunofluorescence with antibodies against EGFP (green) and HA (red). Arrowheads in D,E indicate the cytoplasmic expression of $CCND1^{CAAX}$ and $CCND1^{CAAXK112E}$, respectively. Scale bar: 10 µm. **F**–**H**) Neurons from experiments A-E were analyzed for the relative axon length (F), the relative neurite length (G) and the neurite number per neuron (H) using the NeuronJ plugin of ImageJ. Values are expressed as mean ± SEM ($n = 3$ experiments, > 25 neurons/experiment). Significance was determined by one-way ANOVA and Tukey-HSD post-hoc test (*$p < 0.05$;**$p < 0.01$). **I**-**K**) Cultures of mouse cortical neurons were co-transfected before seeding with plasmids encoding either scramble (scrbl) or *Ccnd1* shRNA ($sh.^{Ccnd1}$) and a plasmid encoding EGFP, as indicated. After 1 DIV, cultures were fixed and analyzed by immunofluorescence with antibodies against EGFP. Relative axon length (I), relative neurite length (J) and the neurite number per neuron (K) were analyzed using the NeuronJ plugin of ImageJ. Values are expressed as mean ± SEM ($n = 3$ experiments, > 25 neurons/experiment). Significance was determined by one-way ANOVA and Tukey-HSD post-hoc test (*$p < 0.05$;**$p < 0.01$)

In the present work we show that CCND1 is present in the RGP of progenitor cells during cortex development, in vivo, and that is associated to b1-integrin at the plasma membrane of the tip of the basal RGP. This cytoplasmic localization was previously reported for CCND2, being important for the regulation of asymmetric cell division during corticogenesis and neuronal differentiation [15, 51]. In contrast to our results, this localization was not previously observed for CCND1 [15], probably due to the use of different CCND1 antibodies or different tissue preparation protocols. *Ccnd2* mRNA requires a unique cis-regulatory sequence in its 3' untranslated region to be transported into the RGP, where is locally translated [51]. We have been unable to detect a similar sequence in the *Ccnd1* mRNA and therefore the mechanisms regulating cytoplasmic localization of CCND1 remain to be elucidated.

Our data indicate that cytoplasmic CCND1 expression in radial glial cells needs to be tightly regulated to achieve proper pallium formation and layering. Overexpression of cytoplasmic CCND1 accelerates their detachment from the

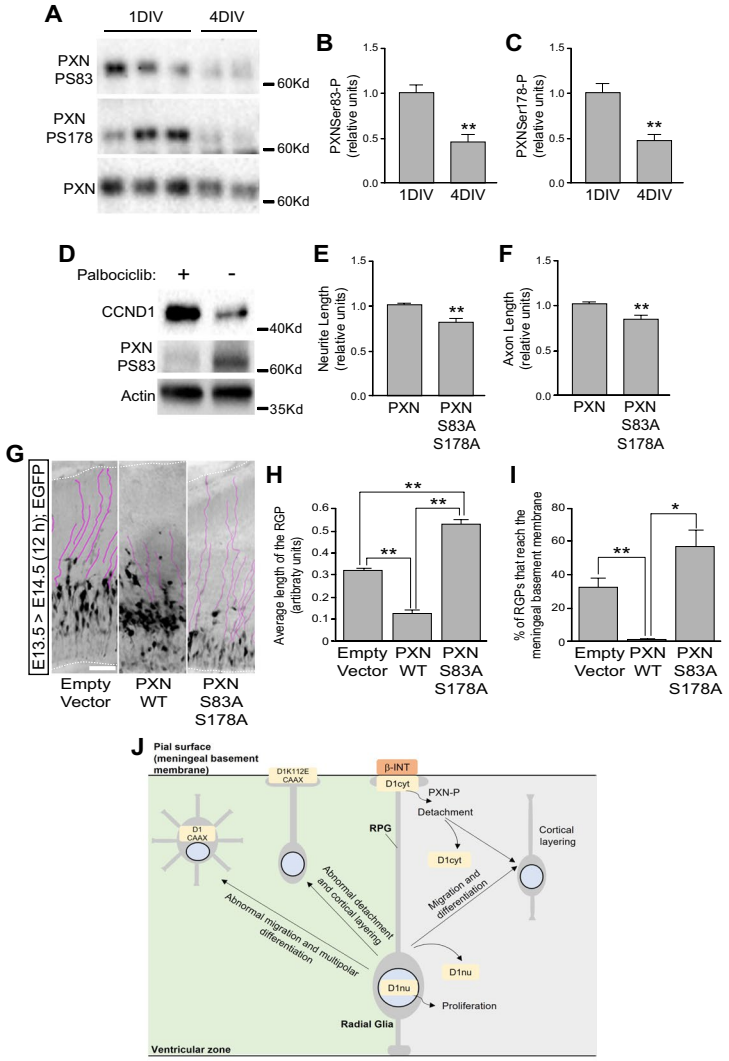

Fig. 7 Phosphorylation of paxillin is mediated by CCND1/CDK and is required for neuron differentiation in vitro, and for RGP detachment from the meningeal basement membrane in vivo. **A**) Western-blot analysis of the phosphorylation of paxillin (PXN) on protein extracts from cortical neuron cultures after 1 or 4 DIV with specific phospho antibodies (phospho-serine83, PS83, upper panel; phosphor-serine178, PS178, middle panel). Lower panel in A show the total levels of paxillin. **B** and **C**) Quantification of the phosphorylation of paxillin in A was corrected by the total paxillin levels and values are expressed as mean ± SEM ($n = 3$). Significance was determined by *t*-Student (**$p < 0.01$). B) Quantification of phosphorylation at serine 83. C) Quantification of phosphorylation at serine 178. **D**) Representative Western-blot analysis of the phosphorylation of paxillin (phospho-serine 83, PS83, middle panel) on hippocampal slices in the presence of the CDK4/6 inhibitor palbociclib (2.5 µM), as indicated. Upper and lower panels show the levels of CCND1 and actin, respectively. **E** and **F**) Cortical neuron cultures were co-electroporated as in Fig. 6 (A-H) with wild-type paxillin (PXN) or the non-phosphorylatable paxillin (PXNS83AS178A), respectively and a plasmid encoding EGFP and were analyzed after 1 DIV for the relative neurite (E) and axon (F) length. Values are expressed as mean ± SEM ($n = 3$ experiments, > 25 neurons/experiment). Significance was determined by *t*-Student (**$p < 0.01$). **G**) Representative images of the pallium IUE at E13.5 with paxillin wild-type (PXN WT), the non-phosphorylatable paxillin (PXNS83AS178A) or the empty vector control (pCAGIG), as indicated and analyzed at E14.5, 12 h later. RGP were highlighted by purple lines. Scale bar: 100 µm. **H** and **I**) Quantification of the average RGP length (H) or the percentage of RGP attached to the meningeal basement membrane (I) in the conditions described in panel G. Values are expressed as mean ± SEM ($n = 3$ embryos; > 30 processes per experimental condition for each embryo). Significance was determined by one-way ANOVA and Tukey-HSD post-hoc test (*$p < 0.05$;**$p < 0.01$). **J**) Summary of our results. Right part (light grey): during normal cortex development CCND1 needs to be downregulated both from the nucleus (D1nu) and from the RGP (D1cyt) of cortical progenitors to stop cell division and to allow migration and differentiation and to detach from the meningeal basement membrane, respectively. In the later case, phosphorylation of paxillin (PXN-P) by cytoplasmic CCND1/CDK complexes is required. Left part (light green): expression of cytoplasmic CCND1 (D1CAAX) triggers abnormal migration and multipolar shape of differentiating neurons while expression of a dominant negative CCND1, with cytoplasmic localization (D1K112E-CAAX), triggers abnormal detachment of RGP from the meningeal basement membrane and layering defects

meningeal basement membrane and affects the morphology and the positioning of post-mitotic neurons while expression of a dominant negative mutant delays this detachment and cause mispositioning of TBR2+progenitors and CTIP2+neurons. Some of these layering defects were also observed in *Ccnd1* knock-out brains, highlighting the importance of cytoplasmic CCND1 in vivo. Acute experiments by IUE with the dominant negative mutant show indeed stronger effects than the knock-out, suggesting a broader inhibition of CDKs. Most of the interactors and signalling effectors of cytoplasmic CCND1 have been related to cell adhesion at the plasma membrane, including the actin-binding protein filamin A in membrane ruffles [53], the cytoplasmic adapter protein PACSIN 2 in focal adhesions [31], the RAL GTPases [5, 8] and paxillin, a downstream integrin signalling protein in focal adhesions [12]. Here we provide evidence that cytoplasmic CCND1 in radial glial cells could be regulating cortex development by integrin signalling through paxillin phosphorylation, adding evidence of the important role of integrin signalling in this process [27]. We have shown that CCND1 co-localizes with β1-integrin at the plasma membrane of the distal tip of the basal RGP, that CCND1 levels correlate with phosphorylation of paxillin in neurons and that this phosphorylation is necessary for neurite extension, in vitro, and for detachment of the RGP from the meningeal membrane, in vivo. Proper detachment of RGP from the meningeal basement membrane has been shown to be essential for cortical layering. For instance, deletion of β 1-integrin from progenitor cells, but not from post-mitotic neurons, triggers abnormal development of the glial end feet, disruption of the basal lamina and perturbs cortical layer formation, mainly affecting upper layers [2, 17]. In addition, interference with the adhesion protein TAG-1 (transient axonal glycoprotein-1), also known as contactin-2, provokes basal RGP retraction leading to cortical layering defects including ectopic TBR2+progenitors and CTIP2+cells mislocalization [36]. By contrast, we report an opposite correlation between increased RGP adhesion and layering defects. This might be due to differences in the developmental stage where the experiments were performed. Although speculative and in need of further investigation, it is also possible that exact detachment timing of the RGP from the meningeal basement membrane is essential for pallium layering and that an acceleration or delay will end up in similar layering defects. Maybe longer adhesion shifts the migration type from locomotion to translocation [34], explaining the increase in the CP of electroporated neurons bearing the CCND1 dominant negative mutant and the concomitant layering defects.

Although the cytoplasmic expression of CCND1 was mostly observed in the RGP we cannot rule out that significant amounts of cytoplasmic CCND1 could play a role as well in post-mitotic neurons, as previously suggested [29, 37, 47, 49]. Paxillin or β1-integrin knock-out animals display a delay in positioning of upper layer neurons, a cell-autonomous effect in post-mitotic neurons triggered by changes in neuron morphology and by a slower migration [41, 42]. A similar phenotype was observed by ablation of focal adhesion kinase (FAK), which is recruited by paxillin into focal adhesions, reinforcing the role of integrin signalling in post-mitotic neurons during cortex formation [52]. According to this data, it is possible that activation of paxillin by CCND1 accelerates migration, explaining therefore the accumulation of neurons in the CP upon cytoplasmic CCND1 overexpression. Finally, there is also the possibility that other substrates of cytoplasmic CCND1/CDK activity, different from paxillin, could have a role during cortex development.

In summary, our results provide evidence for a novel function of the cytoplasmic CCND1 in cortical brain development which is independent of its canonical role on cell cycle regulation and involves the control of integrin signaling and cell adhesion of the RGPs to the meningeal basement membrane.

Supplementary Information The online version contains supplementary material available at https://doi.org/10.1007/s00018-026-06178-1.

Acknowledgements Acknowledgements: We thank the funding agencies Ministerio de Ciencia, Innovación y Universidades, Plan Estatal de Investigación Científica y Técnica y de Innovación (Egea: PGC2018-101910-B-I00 and PID2021-129089NB-I00; Garí/Ferrezuelo: PID2019-104859GB-I00) and the Generalitat de Catalunya, Agència de Gestió d'Ajuts Universitaris i de Recerca (AGAUR), Suport Grups de Recerca SGR2021, 01113 (Garí). We thank members of the Cell Cycle and the Oncogenic and Developmental Signaling groups for fruitful discussions. Special thanks to Sònia Rius for technical support and to Jèssica Pairada and the rest of the animal facility and the tissue culture staff of the University of Lleida, for technical service.

Authors contributions Neus Pedraza, designed and performed research, analysed data and wrote the paper.
Daniel Rocandio, designed and performed research, analysed data.
Bahira Zammou, performed research.
Maria Ventura Monserrat, performed research.
Ariadna Ortiz-Brugués, performed research.
Pau Marfull-Oromí, performed research.
Disha Chauhan, performed research.
Mario Encinas, analysed data.
Xavier Dolcet, analysed data.
Francisco Ferrezuelo, designed, analysed data and wrote the paper.
Eloi Garí, designed, analysed data and wrote the paper.
Joaquim Egea, designed and performed research, analysed data and wrote the paper.

Funding Open Access funding provided thanks to the CRUE-CSIC agreement with Springer Nature. This work was supported by the funding agencies Ministerio de Ciencia, Innovación y Universidades, Plan Estatal de Investigación Científica y Técnica y de Innovación (Egea: PGC2018-101910-B-I00 and PID2021-129089NB-I00; Garí/Ferrezuelo: PID2019-104859 GB-I00) and the Generalitat de Catalunya, Agència de Gestió d'Ajuts Universitaris i de Recerca (AGAUR), Suport Grups de Recerca SGR2021, 01113 (Garí).

Data availability The datasets generated during and/or analysed during the current study are available under request to the corresponding author.

Declarations

Ethics approval Animal care followed the Guidelines of the University of Lleida for Animal Experimentation in accordance with Catalan, Spanish, and European Union regulations (Decret 214/1997, Real Decreto 53/2013, and Directive 63/2010).

Consent to participate and consent to publish Not applicable.

Competing interests The authors have no relevant financial or non-financial interests to disclose.

Open Access This article is licensed under a Creative Commons Attribution 4.0 International License, which permits use, sharing, adaptation, distribution and reproduction in any medium or format, as long as you give appropriate credit to the original author(s) and the source, provide a link to the Creative Commons licence, and indicate if changes were made. The images or other third party material in this article are included in the article's Creative Commons licence, unless indicated otherwise in a credit line to the material. If material is not included in the article's Creative Commons licence and your intended use is not permitted by statutory regulation or exceeds the permitted use, you will need to obtain permission directly from the copyright holder. To view a copy of this licence, visit http://creativecommons.org/licenses/by/4.0/.

References

1. Artegiani B, Lindemann D, Calegari F (2011) Overexpression of cdk4 and cyclinD1 triggers greater expansion of neural stem cells in the adult mouse brain. J Exp Med 208(5):937–948
2. Belvindrah R, Graus-Porta D, Goebbels S, Nave KA, Müller U (2007) Beta1 integrins in radial glia but not in migrating neurons are essential for the formation of cell layers in the cerebral cortex. J Neurosci 27(50):13854–13865
3. Borello U, Berarducci B, Delahaye E, Price DJ, Dehay C (2018) SP8 transcriptional regulation of cyclin D1 during mouse early corticogenesis. Front Neurosci 12:119
4. Bragado Alonso S, Reinert JK, Marichal N, Massalini S, Berninger B, Kuner T, Calegari F (2019) An increase in neural stem cells and olfactory bulb adult neurogenesis improves discrimination of highly similar odorants. EMBO J 15;38(6):e98791
5. Cemeli T, Guasch-Vallés M, Nàger M, Felip I, Cambray S, Santacana M, Gatius S, Pedraza N, Dolcet X, Ferrezuelo F, Schuhmacher AJ, Herreros J, Garí E (2019) Cytoplasmic cyclin D1 regulates glioblastoma dissemination. J Pathol 248(4):501–513
6. Ciemerych MA, Kenney AM, Sicinska E, Kalaszczynska I, Bronson RT, Rowitch DH, Gardner H, Sicinski P (2002) Development of mice expressing a single D-type cyclin. Genes Dev 16(24):3277–3289
7. Delaunay D, Kawaguchi A, Dehay C, Matsuzaki F (2017) Division modes and physical asymmetry in cerebral cortex progenitors. Curr Opin Neurobiol 42:75–83
8. Fernández RM, Ruiz-Miró M, Dolcet X, Aldea M, Garí E (2011) Cyclin D1 interacts and collaborates with Ral GTPases enhancing cell detachment and motility. Oncogene 30(16):1936–1946
9. Fernández-Hernández R, Rafel M, Fusté NP, Aguayo RS, Casanova JM, Egea J, Ferrezuelo F, Garí E (2013) Cyclin D1 localizes in the cytoplasm of keratinocytes during skin differentiation and regulates cell-matrix adhesion. Cell Cycle 12(15):2510–2517
10. Fleitas C, Marfull-Oromí P, Chauhan D, Del Toro D, Peguera B, Zammou B, Rocandio D, Klein R, Espinet C, Egea J (2021) FLRT2 and FLRT3 cooperate in maintaining the tangential migratory streams of cortical interneurons during development. J Neurosci 41(35):7350–7362
11. Flora A, Klisch TJ, Schuster G, Zoghbi HY (2009) Deletion of Atoh1 disrupts Sonic Hedgehog signaling in the developing cerebellum and prevents medulloblastoma. Science 326(5958):1424–1427
12. Fusté NPa, Fernández-Hernández R, Cemeli T, Mirantes C, Pedraza N, Rafel M, Torres-Rosell J, Colomina N, Ferrezuelo F, Dolcet X, Garí E (2016) Cytoplasmic cyclin D1 regulates cell invasion and metastasis through the phosphorylation of paxillin. Nat Commun 7:11581
13. Fusté NPb, Castelblanco E, Felip I, Santacana M, Fernández-Hernández R, Gatius S, Pedraza N, Pallarés J, Cemeli T, Valls J, Tarres M, Ferrezuelo F, Dolcet X, Matias-Guiu X, Garí E (2016) Characterization of cytoplasmic cyclin D1 as a marker of invasiveness in cancer. Oncotarget 7(19):26979–26991
14. Gao J, Liao J (2009) Yang GY (2009) CAAX-box protein, prenylation process and carcinogènesis. Am J Transl Res 1(3):312–325
15. Glickstein SB, Alexander S, Ross ME (2007) Differences in cyclin D2 and D1 protein expression distinguish forebrain progenitor subsets. Cereb Cortex 17(3):632–642
16. Glickstein SB, Monaghan JA, Koeller HB, Jones TK, Ross ME (2009) Cyclin D2 is critical for intermediate progenitor cell proliferation in the embryonic cortex. J Neurosci 29(30):9614–9624
17. Graus-Porta D, Blaess S, Senften M, Littlewood-Evans A, Damsky C, Huang Z, Orban P, Klein R, Schittny JC, Müller U (2001) Beta1-class integrins regulate the development of laminae and folia in the cerebral and cerebellar cortex. Neuron 31(3):367–379
18. Hagey DW, Topcic D, Kee N, Reynaud F, Bergsland M, Perlmann T, Muhr J (2020) CYCLIN-B1/2 and -D1 act in opposition to coordinate cortical progenitor self-renewal and lineage commitment. Nat Commun 11:2898
19. Halterman MW, Giuliano R, Dejesus C, Schor NF (2009) In-tube transfection improves the efficiency of gene transfer in primary neuronal cultures. J Neurosci Methods 177(2):348–354
20. Hancock JF (2003) Ras proteins: different signals from different locations. Nat Rev Mol Cell Biol 4(5):373–84. https://doi.org/10.1038/nrm1105
21. Hiraiwa A, Matsui K, Nakayama Y, Komatsubara T, Magara S, Kobayashi Y, Hojo M, Kato M, Yamamoto T, Tohyama J (2021) Polymicrogyria with calcification in Pallister-Killian syndrome detected by microarray analysis. Brain Dev 43(3):448–453
22. Huard JM, Forster CC, Carter ML, Sicinski P, Ross ME (1999) Cerebellar histogenesis is disturbed in mice lacking cyclin D2. Development 126(9):1927–1935
23. Hydbring P, Malumbres M, Sicinski P (2016) Non-canonical functions of cell cycle cyclins and cyclin-dependent kinases. Nat Rev Mol Cell Biol 17(5):280–292
24. Kenney AM, Rowitch DH (2000) Sonic hedgehog promotes G(1) cyclin expression and sustained cell cycle progression in mammalian neuronal precursors. Mol Cell Biol 20(23):9055–9067
25. Landis MW, Pawlyk BS, Li T, Sicinski P, Hinds PW (2006) Cyclin D1-dependent kinase activity in murine development and mammary tumorigenesis. Cancer Cell 9(1):13–22
26. Lange C, Huttner WB, Calegari F (2009) Cdk4/cyclinD1 overexpression in neural stem cells shortens G1, delays neurogenesis, and promotes the generation and expansion of basal progenitors. Cell Stem Cell 5(3):320–331
27. Long KR, Huttner WB (2019) How the extracellular matrix shapes neural development. Open Biol 9(1):180216

28. Lukaszewicz A, Savatier P, Cortay V, Giroud P, Huissoud C, Berland M, Kennedy H, Dehay C (2005) G1 phase regulation, area-specific cell cycle control, and cytoarchitectonics in the primate cortex. Neuron 47(3):353–364
29. Lukaszewicz AI, Anderson DJ (2011) Cyclin D1 promotes neurogenesis in the developing spinal cord in a cell cycle-independent manner. Proc Natl Acad Sci USA 108(28):11632–11637
30. Marampon F, Casimiro MC, Fu M, Powell MJ, Popov VM, Lindsay J, Zani BM, Ciccarelli C, Watanabe G, Lee RJ, Pestell RG (2008) Nerve growth factor regulation of cyclin D1 in PC12 cells through a p21RAS extracellular signal-regulated kinase pathway requires cooperative interactions between Sp1 and nuclear factor-kappaB. Mol Biol Cell 19(6):2566–2578
31. Meng H, Tian L, Zhou J, Li Z, Jiao X, Li WW, Plomann M, Xu Z, Lisanti MP, Wang C, Pestell RG (2011) PACSIN 2 represses cellular migration through direct association with cyclin D1 but not its alternate splice form cyclin D1b. Cell Cycle 10(1):73–81
32. Mirzaa G, Parry DA, Fry AE, Giamanco KA, Schwartzentruber J, Vanstone M, Logan CV, Roberts N, Johnson CA, Singh S, Kholmanskikh SS, Adams C, Hodge RD, Hevner RF, Bonthron DT, Braun K, Faivre L, Riviére JB, St-Onge J, Gripp KW, Braun KPJ, Mancini GM, Pang K, Sweeney E, van Esch H, Verbeek N, Wieczorek D, Steinraths M, Majewski J, Boycot KM, Pilz DT, Ross ME, Dobyns WB, Sheridan EG (2014) De novo CCND2 mutations leading to stabilization of cyclin D2 cause megalencephaly-polymicrogyria-polydactyly-hydrocephalus syndrome. Nat Genet 46(5):510–515
33. Miyashita S, Owa T, Seto Y, Yamashita M, Aida S, Sone M, Ichijo K, Nishioka T, Kaibuchi K, Kawaguchi Y, Taya S, Hoshino M (2021) Cyclin D1 controls development of cerebellar granule cell progenitors through phosphorylation and stabilization of ATOH1. EMBO J 40(14):e105712
34. Nadarajah B, Brunstrom JE, Grutzendler J, Wong RO, Pearlman AL (2001) Two modes of radial migration in early development of the cerebral cortex. Nat Neurosci 4(2):143–150
35. Najas S, Arranz J, Lochhead PA, Ashford AL, Oxley D, Delabar JM, Cook SJ, Barallobre MJ, Arbonés ML (2015) DYRK1A-mediated cyclin D1 degradation in neural stem cells contributes to the neurogenic cortical defects in Down syndrome. EBioMedicine 2(2):120–134
36. Okamoto M, Namba T, Shinoda T, Kondo T, Watanabe T, Inoue Y, Takeuchi K, Enomoto Y, Ota K, Oda K, Wada Y, Sagou K, Saito K, Sakakibara A, Kawaguchi A, Nakajima K, Adachi T, Fujimori T, Ueda M, Hayashi S, Kaibuchi K, Miyata T (2013) TAG-1-assisted progenitor elongation streamlines nuclear migration to optimize subapical crowding. Nat Neurosci 16(11):1556–1566
37. Pedraza N, Monserrat MV, Ferrezuelo F, Torres-Rosell J, Colomina N, Miguez-Cabello F, Párraga JP, Soto D, López-Merino E, García-Vilela C, Esteban JA, Egea J, Garí E (2023) Cyclin D1-Cdk4 regulates neuronal activity through phosphorylation of GABAA receptors. Cell Mol Life Sci 80(10):280
38. Pilaz LJ, Patti D, Marcy G, Ollier E, Pfister S, Douglas RJ, Betizeau M, Gautier E, Cortay V, Doerflinger N, Kennedy H, Dehay C (2009) Forced G1-phase reduction alters mode of division, neuron number, and laminar phenotype in the cerebral cortex. Proc Natl Acad Sci U S A 106(51):21924–21929
39. Pirozzi F, Lee B, Horsley N, Burkardt DD, Dobyns WB, Graham JM, Dentici ML, Cesario C, Schallner J, Porrmann J, Di Donato N, Sanchez-Lara PA, Mirzaa GM (2022) Proximal variants in CCND2 associated with microcephaly, short stature, and developmental delay: a case series and review of inverse brain growth phenotypes. Am J Med Genet A 185(9):2719–2738
40. Pogoriler J, Millen K, Utset M, Du W (2006) Loss of cyclin D1 impairs cerebellar development and suppresses medulloblastoma formation. Development 133(19):3929–3937
41. Rashid M, Belmont J, Carpenter D, Turner CE, Olson EC (2017) Neural-specific deletion of the focal adhesion adaptor protein paxillin slows migration speed and delays cortical layer formation. Development 144(21):4002–4014
42. Rashid M, Olson EC (2023) Delayed cortical development in mice with a neural specific deletion of β1 integrin. Front Neurosci 17:1158419
43. Satyanarayana A, Kaldis P (2009) Mammalian cell-cycle regulation: several Cdks, numerous cyclins and diverse compensatory mechanisms. Oncogene 28(33):2925–2939
44. Schmetsdorf S, Gärtner U, Arendt T (2005) Expression of cell cycle-related proteins in developing and adult mouse hippocampus. Int J Dev Neurosci 23(1):101–112
45. Sherr CJ (1993) Mammalian G1 cyclins. Mammalian G1 cyclins. Cell 73(6):1059–1065
46. Sicinski P, Donaher JL, Parker SB, Li T, Fazeli A, Gardner H, Haslam SZ, Bronson RT, Elledge SJ, Weinberg RA (1995) Cyclin D1 provides a link between development and oncogenesis in the retina and breast. Cell 82(4):621–630
47. Song L, Tian X, Schekman R (2021) Extracellular vesicles from neurons promote neural induction of stem cells through cyclin D1. J Cell Biol 220(9):e202101075
48. Sumrejkanchanakij P, Eto K, Ikeda MA (2006) Cytoplasmic sequestration of cyclin D1 associated with cell cycle withdrawal of neuroblastoma cells. Biochem Biophys Res Commun 340(1):302–328
49. Sumrejkanchanakij P, Tamamori-Adachi M, Matsunaga Y, Eto K, Ikeda MA (2003) Role of cyclin D1 cytoplasmic sequestration in the survival of postmitotic neurons. Oncogene 22(54):8723–8730
50. Takahashi T, Nowakowski RS, Caviness VS Jr (1995) The cell cycle of the pseudostratified ventricular epithelium of the embryonic murine cerebral wall. J Neurosci 15(9):6046–6057
51. Tsunekawa Y, Britto JM, Takahashi M, Polleux F, Tan SS, Osumi N (2012) Cyclin D2 in the basal process of neural progenitors is linked to non-equivalent cell fates. EMBO J 31(8):1879–1892
52. Valiente M, Ciceri G, Rico B, Marín O (2011) Focal adhesion kinase modulates radial glia-dependent neuronal migration through connexin-26. J Neurosci 31(32):11678–11691
53. Zhong Z, Yeow WS, Zou C, Wassell R, Wang C, Pestell RG, Quong JN, Quong AA (2010) Cyclin D1/cyclin-dependent kinase 4 interacts with filamin A and affects the migration and invasion potential of breast cancer cells. Cancer Res 70(5):2105–2114

Publisher's Note Springer Nature remains neutral with regard to jurisdictional claims in published maps and institutional affiliations.